compressive stressor tends to expand when it is released from a thick substrate, the membrane gets deflected and becomes tensile strained as shown in Fig. 1(b).
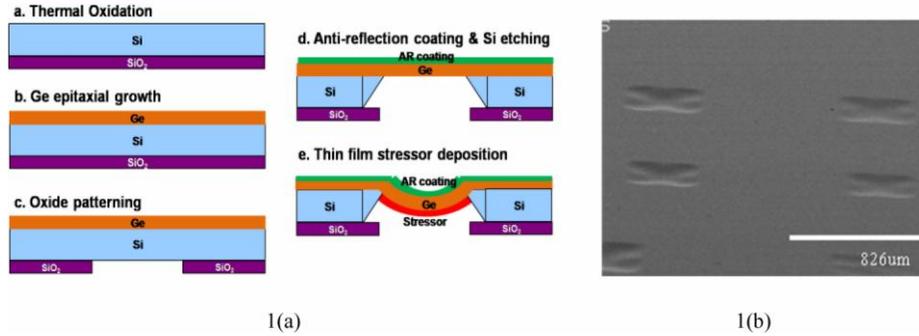

Fig. 1. (a) Fabrication process flow for highly strained Ge membrane (b) SEM picture of deflected membranes

3. Optical properties

A biaxial tensile strain larger than 1% was measured from both room temperature photoluminescence (PL) and Raman spectroscopy measurements. The excitation wavelengths were 532nm and 514nm for PL and Raman spectroscopy measurements, respectively. Both measurements were conducted at room temperature and the laser excitation power on the sample for PL was approximately 10mW. A strained InGaAs detector cooled to −100°C by liquid nitrogen was used to perform the measurements over an extended wavelength range.
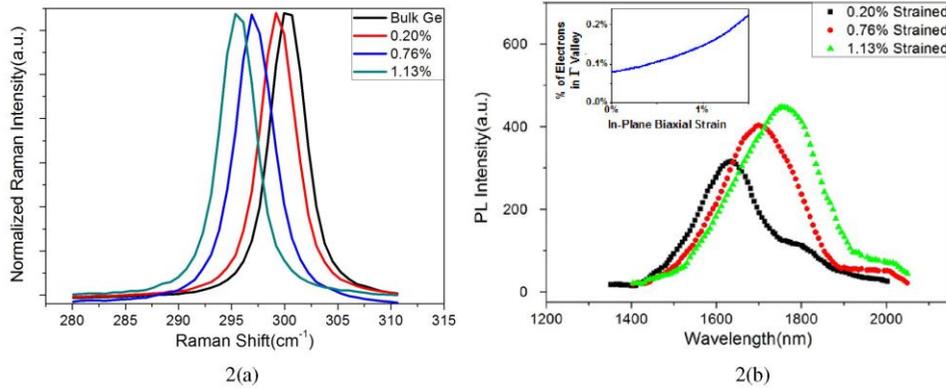

Fig. 2. (a) Normalized Raman spectra (b) Room temperature direct band gap PL spectra. The inset of the figure(b) shows how the percentage of electrons in the Γ valley increases with strain according to our simulations.

In Fig. 2(a), Raman spectroscopy measurements show the amount of bi-axial tensile strain in four different samples, crystalline Ge and Ge membranes with no stressor, 500nm, and 900nm tungsten stressor layers. Compared to crystalline Ge, the peak position shifts to the left as tensile strain is introduced in Ge membranes by thermal expansion mismatch for free standing membrane. The peak shifts even further by depositing thicker stressor layers. According to the equation for strain calculation from ref [26], the samples with 500nm and 900nm tungsten are under 0.76% ± 0.10% and 1.13% ± 0.13% biaxial tensile strain, respectively, where the errors are due to the resolution limit of the setup.

Photoluminescence measurements also confirmed a large tensile strain in our membrane as shown in Fig. 2(b). The dominant peaks are due to the transition from the direct Γ valley to the heavy-hole band [12,13]. Figure 2(b) shows the peak wavelengths of 1620nm, 1690nm

and 1750nm for a free standing and strained membranes, respectively. Moreover, the integrated PL intensity from the 1.13% strained membrane is approximately twice as large as from the 0.2% strained membrane. The inset of Fig. 2(b) shows how the percentage of electrons in the Γ valley increases with strain, assuming heavy n-doping. This is because higher strain lowers the Γ valley edge relative to the L valley edge, thereby increasing spillover from the L valley into the Γ valley. Since the PL spectrum is dominated by transitions from the gamma valley, we expect the increase in gamma valley population to be roughly proportional to the integrated intensity of the PL signal. Comparing the 0.2% strained and 1.13% strained cases, our theoretical modeling of a 2x increase in Γ valley population is in good agreement with our experimental results which show approximately a 2x higher integrated PL intensity.
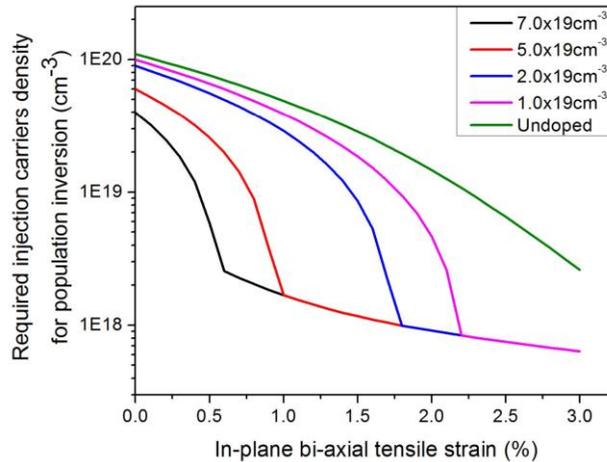

Fig. 3. Required injection carrier density for population inversion versus strain for different n-type doping concentration.

Looking toward future lasing applications, population inversion in Ge is much more readily achievable with a combination of n-doping, which begins filling the L-valley, and strain, which lowers the Γ-valley and also reduces the density of states in certain bands, notably the valence band. To quantify these changes, we have used sp3d5s* tight-binding with spin-orbital coupling [20], which incorporates diagonal parameter shifts due to the nearest-neighbor interactions when strain is present [21], to calculate the full band structure. From there, the carrier concentrations were approximated by summing the contributions from a mesh of evenly-spaced k-points over the entire first Brillouin zone. As shown in Fig. 3, our simulations predict that a combination of strain and n-doping would drastically reduce the amount of pumping required for population inversion (i.e. electron quasi-Fermi level within the gamma valley, and hole quasi-Fermi level within the valence band). While an undoped and unstrained Ge membrane would require pumping of $1.1 \times 10^{20} cm^{-3}$ to achieve population inversion, 1.1%-strained and $5 \times 10^{19} cm^{-3}$ n-doped Ge requires pumping of only $1.6 \times 10^{18} cm^{-3}$, a reduction of nearly two orders of magnitude. Note that the curves for n-doped Ge in Fig. 3 saturate to a lower bound with increased strain; this represents the region where the electron quasi-Fermi level is already near or above the Γ-valley, and so the required pumping is determined by how many carriers are needed to push the hole quasi-Fermi level down to the top of the valence band. Since n-type dopant activation in Ge higher than $5 \times 10^{19} cm^{-3}$ is readily achievable by either coimplantation of Sb and P [27] or laser annealing [28], our technique for larger than 1% strain strengthens the possibility of Ge laser for on-chip interconnects. It should also be noted that our simulations predict a crossover of the direct bandgap at roughly 2.2% strain, whereas most theoretical predictions claim the crossover

occurs around 1.7-1.9% strain [6–8] and low-temperature PL experiments have suggested that 1.8% strain is already sufficient for a direct bandgap at 5K [29]. In addition, there is some error introduced by approximating the carrier density by summing over a finite number of k-points. However, increasing the density (and accuracy) of the mesh of k-points tends to return slightly lower carrier densities in all valleys, which would increase the enhancement from n-doping. Thus, our simulations are likely understating both the enhancement from strain and the enhancement from n-doping, and so these results should be viewed as pessimistic estimates.

4. Device realization

Vertical PN photodetectors (PDs) were fabricated on highly strained membranes to show the possibility of device integration using our technique. Figure 4(a) shows a schematic cross-section of a strained Ge PN photodetector. A 1.4µm undoped Ge and 250nm n$^+$-Ge layer is grown epitaxially using diluted 1% phosphine in situ doping without a subsequent annealing to avoid phosphorous dopant diffusion. A 450nm high Ge mesa is then patterned by dry etching, leaving p-type Ge as a supporting layer for a thin Ge membrane structure. Ti/Al metal contacts are realized by lift-off method for both n and p-type contacts. With a protective coating on the top surface, the Si substrate is etched and tungsten is deposited from the backside in order to introduce a higher strain. Figure 4(b) is an image from optical microscope showing a strained PD.
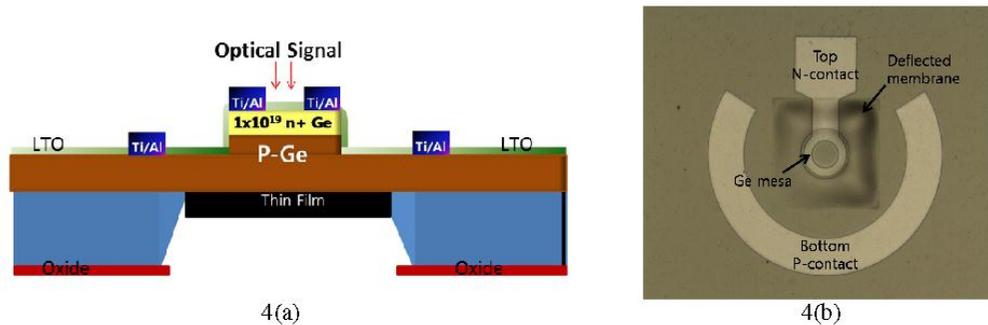

Fig. 4. (a) Schematic diagram of strained Ge PN photodetector (b) Optical image of a strained PD showing a deflected active region

The photocurrent measurement was conducted by shining light from a tunable optical parametric oscillator on the center of the mesa while the device was under 1V bias. Figure 5 shows the normalized photocurrent spectra from three different samples with 0.2%, 0.58%, and 0.76% bi-axial tensile strain. The device with a 0.2% strained active region shows a roll-off of the measured photocurrent below 1.6um due to the direct band gap in Ge. Notably, PDs with both 0.58% and 0.76% bi-axial tensile strain show an excellent responsivity well beyond 1.6um. This effect can be attributed to the direct band gap reduction in Ge resulting in an enhanced absorption for longer wavelengths. Multiple peaks at around 1.55µm and 1.7µm are due to the Fabry-Perot cavity enhancement from the free-standing Ge membrane and the inset shows the calculated enhancement factor in the 1.65µm Ge membrane PD using the transfer matrix method [30]. We are currently investigating electroluminescence from this highly-strained Ge diode in the hopes of improving the efficiency of Ge light emitting diodes (LEDs). A benefit of the circular geometry is that whispering gallery modes should be readily available as we move toward a strained-Ge laser.
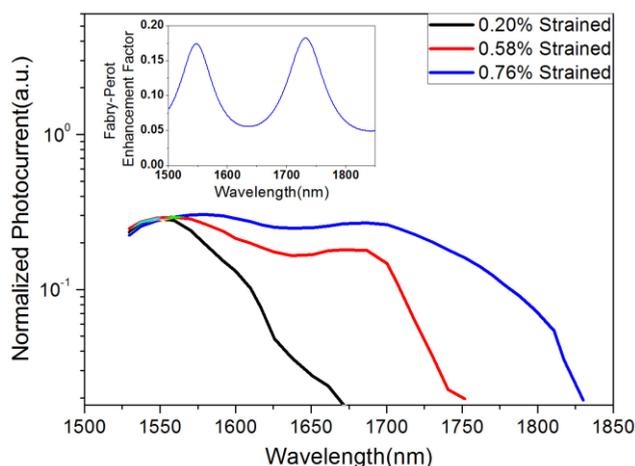
Fig. 5. Normalized photocurrents from strained PDs showing the extended responsivity beyond 1.6um due to the bandgap reduction. Inset shows the calculated Fabry-Perot enhancement factors in a 1.65um Ge membrane, assuming a complex refractive index of n = 4.35, k = 0.01.

5. Conclusion

We have proposed and demonstrated a method to fabricate a thin Ge membrane integrated on a Si substrate and induce a sustainable and large tensile strain by depositing a stressor layer to improve the Ge's optical properties. From room temperature photoluminescence and Raman spectroscopy measurement, larger than 1% biaxial tensile strain is confirmed in highly strained membranes and a direct band gap energy reduction of 100meV is observed. Light emission efficiency from the 1.13% strained membrane was significantly improved compared to the 0.2% strained membrane, as predicted in our simulation for the fraction of electrons in the Γ valley vs. strain. According to our tight-binding calculations, population inversion in 1% strained and heavily doped Ge can be achieved with two orders of magnitude less injection than unstrained and undoped Ge. Moreover, we presented the first device fabrication using highly strained Ge and showed an excellent responsivity well beyond 1.6μm from a 0.76% strained Ge photodetector. We believe that our strain-tunable membrane can ultimately be utilized for high efficiency near-infrared lasers, which are essential to realize on-chip optical interconnects.

Acknowledgments